Femtosecond laser induced and controlled chemical reaction of carbon monoxide and hydrogen

A. du Plessis[1,2], C.A. Strydom[2], H Uys[1], A Hendriks[1], GN Botha[1] and L.R. Botha[1]

[1]*CSIR National Laser Centre, Meiring Naude Rd, Pretoria, South Africa*
[2]*School of Physical and Chemical Sciences, North-West University, Potchefstroom, South Africa*

Results from experiments aimed at bimolecular chemical reaction control of CO and H_2 at room temperature and pressure, without any catalyst, using shaped femtosecond laser pulses are presented. A stable reaction product (CO_2) was measured after irradiation by near transform limited pulses, using time of flight mass spectroscopy and confirmed by gas chromatography. This product is confirmed to only be formed when H_2 is also present in the reaction cell. There is also evidence for C-H and C-C bond formation. We present also coherent control experimental results from low pressure time of flight mass spectrometer and the idea that such optimized pulses could be applied to a high pressure reaction cell is a new concept. Although control in this scenario is indirect, through the breaking of bonds and the selective generation of specific ion fragments, the extreme cases of varying intensity and applying an anti-optimum pulse provide evidence that this concept may be useful in chemical reaction control efforts.

Introduction

The choice of reaction

The Fischer-Tropsch reaction of CO and H_2 to produce various hydrocarbons has been one of the most economically relevant industrial catalytic chemical reactions employed on a large scale to date. The most important reactions are those producing alkanes:

$$(2n+1)H_2 + nCO \rightarrow C_nH_{(2n+2)} + nH_2O$$

Where n=1,2,3,… producing CH_4, C_2H_6, C_3H_8, …

The enhancement of the reaction rate, efficiency and improvements in the selectivity of reaction products (especially gearing the production towards high-mass alkanes rather than methane) has been widely studied (Dry et al 2002). These changes are usually induced by a variation of the ratio of reactant gases, the reaction chamber temperature and pressure and by the use of various catalysts (of which Co and Fe are most widely used).

Due to the continuously increasing cost of petrochemical products (including transportation fuels), there is a scientific interest in developing new production technologies for high value hydrocarbon products from this reaction, which may be more selective and therefore require less post-production separation. In addition, a

combination of biomass gasification and Fischer-Tropsch synthesis is a possible route to renewable fuels (Jun et al 2004).

Laser induced and controlled chemical reactions is a research topic of increasing scientific interest, partly due to advances made in laser technology (and in particular femtosecond laser coherent control techniques), but also partly due to the lowering cost and maturing of laser technology. It is only a matter of time before laser induced chemical reactions will be financially competitive with some chemical synthesis methods, especially for high value chemicals and those requiring expensive purification when synthesized by other means.

The Fisher-Tropsch reaction was chosen to illustrate the global potential of this technology, and the technique is by no means limited to this reaction. In fact, this is one of the most difficult reactions to control due to the fact that these molecules are small, have very fast vibrational energy redistribution times (one of the fundamental limits to coherent control) and are not known to be photo-reactive. Many new applications and chemical synthesis techniques may be developed in future using this technology.

Femtosecond laser coherent control

Femtosecond laser adaptive feedback control, also called coherent control, is a technique whereby spectrally and temporally shaped ultrashort pulses are used to control atomic and molecular processes such as the excitation of specific states, molecular dissociation, and many more. For recent reviews, see Brif et al (2010), Brixner et al (2004), Dantus et al (2004) and Lozovoy et al (2006). The principle is that the laser-matter interaction changes when the pulse characteristics change, which allows one potential outcome of the interaction to be “selected” over another one, by changing the pulse parameters. If there are two or more pathways to the selected outcome and these can interfere constructively and destructively, coherent control is possible. A simple example is a laser induced molecular dissociation reaction which has two potential outcomes. By changing the laser pulse shape (by for example generating a double pulse with delay between them), one of these can be selected, thereby providing the experimentalist with selective bond breaking. Of course it is very complex to calculate the required pulse shape for such reactions, therefore the experimental outcome is fed into a computer with an optimization algorithm, which selects various pulses and converges on the required solution by testing various pulse shapes experimentally and making measurements of their effect in the system under study. In the ideal experiment, the experimental solution could then provide information on how the process is controlled, by deducing what the contributions of specific pulse shape parameters are.

Until recently, most work in this field was done on unimolecular processes. These include dissociation reactions, excitations and molecular transformations. In our laboratory we studied the dissociation and ionization of trichloroethane (see du Plessis et al 2010), although without pulse shaping at that time, only open loop variation of chirp.

Bimolecular reaction control using lasers has progressed along two lines of research. In

the first, narrowband laser radiation is used for bond or mode selective excitation. This was studied since the early 1970's with limited success due to the ultrafast intramolecular vibrational redistribution of deposited energy. However, mode selective chemistry has made some advances. One good example is the bimolecular control of the reaction of H_2O with D to produce either H_2 and OD or HD and OH, see Crim et al (1996).

The second line of research in bimolecular laser reaction control has been femtosecond coherent control. As explained above, coherent control has been successfully for a number of unimolecular processes. Yet, despite the success of this, there have been very limited reports of bimolecular reaction control using this technique. The most important reason for this is likely the difficulty in online measurement of products. The first example was reported by Bartels et al (2002), in which phosgene gas (CCl_2O) was produced by optimally shaped femtosecond pulses interacting with CO_2 and CCl_4 in the gas phase at atmospheric pressure. The measurement technique involved online monitoring of reaction products using Raman scattering of a probe pulse. Another recent example is the control of the surface reaction of CO and H_2 on a catalytic surface in a vacuum chamber by Nuernberger et al (2010). They report laser induced reaction on the catalytic surface as well as optimized pulse shapes for selective product formation resulting in improvement of 100% over the unshaped pulse. They demonstrate the formation of C-H bonds, and in particular HCO and H_2CO. Their measurement tool was time of flight mass spectroscopy coupled to a gas-surface interaction region. Their work is very relevant to the work presented here, as it involves the same reactant species and therefore demonstrates that bimolecular control of these reactant species is possible with this technique. The difference between the work reported there and our work presented here, is that no catalyst was used in our experiments. Our sample gas molecules are therefore not aligned as they are on a catalytic surface, and the bonds are not weakened as they are due to interaction with a metal surface. Our goal is to control gas phase reactions at atmospheric pressure conditions, which can possibly be more easily applied to industrial processes. What we present here is the first example of laser induced reaction between these species without a catalyst, the formation of CO_2, as well as C-H and C-C bonds in this manner, as well as open and closed loop control of the dissociative ionization of the reactant species, and application of these to a high pressure cell. This concept of finding optimized pulses under low pressure conditions and applying them to a high pressure cell, eliminates the need for online monitoring of reaction products in real time, making the experimental procedure much simpler.

Experimental setup

Our experimental setup consists of a Coherent Mira 900F producing 100 fs pulses of 10 nm bandwidth (FWHM) at a repetition rate of 76 MHz, which are sent through a Dazzler acousto-optic programmable dispersive filter, before being stretched, amplified and compressed in a regenerative amplifier (Coherent Legend). The amplified pulses typically have pulse durations of 120-130 fs with a maximum pulse energy of 1 mJ, but with timing enhanced to minimise pre and post pulses, this decreases to about 700 μJ, as was done in this work.

A beam-splitter is used to monitor the laser pulse energy as well as second harmonic

generation signals through a BBO crystal, using fast photodiodes. For coherent control experiments, the beam is focused using a 150 mm achromatic lens into the centre of a vacuum chamber time of flight mass spectrometer (reflectron type), which was newly designed by Kore Inc (UK) for our coherent control experiments. The base pressure is typically $5x10^{-8}$ mbar while experiments are done currently with gas effusively bled through a needle valve into the chamber at average chamber pressures in the range of $1x10^{-7}$ up to $5x10^{-6}$ mbar, before space charge effects become noticeable. All experiments reported here were conducted at $1x10^{-6}$ mbar. The extraction pinhole is larger than usual (10 mm diameter with a grid) due to our requirement to find optimized pulses for macroscopic effects, and all ions generated in the focal volume of the laser is therefore detected in the mass spectrum. This is in contrast to many studies where a small extraction pinhole of less than 1 mm is used to select only those ions generated by a specific intensity region of the focus.

Ion signals are recorded on a 500MHz digitizing oscilloscope, and selected ion peak sizes are recorded by computer, or the entire mass spectrum can be recorded directly. Open loop scans of average power, or of any one of the parameters or "knobs" on the Dazzler control panel, can be done automatically by Matlab and data acquisition from the oscilloscope. Initial closed loop control experiments reported here were done with a gradient based search, the Nelder-Mead search algorithm, using the nine amplitude and phase parameters of the Dazzler control panel simultaneously as its search space. In amplitude this refers to the bandwidth of the shaping window, the central wavelength of the shaping window, a hole in the spectrum with variable central wavelength, width and depth. In phase this refers to the first four coefficients of a Taylor expansion of the phase. Optimization of second harmonic generation was done as a test of the ability of the algorithm to find a solution.

Optimization of ion peaks in the time of flight mass spectrum of carbon monoxide and hydrogen was done under vacuum conditions. Optimized pulses were then applied for fixed time periods to a reaction cell containing the same gases at 1 bar pressure and typically 25% CO and 75% H_2. A sample of this gas was taken by syringe and analyzed in the same time of flight mass spectrometer at 1×10^{-6} mbar, using a transform limited pulse for ionization as analysis tool. In addition a gas chromatograph was used for confirmation of stable reaction products.

Experimental results

(a) Intensity variation and saturation

Femtosecond laser ionization mass spectra from CO and from H_2 with near transform limited pulses of 120 fs, 0.7 mJ and 795 nm focused using a 150 mm achromatic lens, are shown in Figures 1 and 2. The gas is effusively bled into the chamber at an average pressure of $1x10^{-6}$ mbar, while the base pressure is $5x10^{-8}$ mbar. In the CO mass spectrum, the dominant ion is the CO^+ ion. Also seen are ion fragments O^+ and C^+ which are due to the Coulomb explosion of CO^+ or CO^{++}, evidence of Coulomb explosion is seen in the form of split peaks for these species. Similarly, Coulomb explosion fragments O^{++} and C^{++} are observed. H_2O^+ is also seen, and is due to background water vapour in the chamber. CO^{++} is also visible. In the much simpler H_2

mass spectrum, only two peaks are seen, those of H_2^+ and H^+. In comparison to CO, much more dissociation occurs since the H^+ ion is dominant. Although this peak could have a contribution from H_2^{++}, no evidence for Coulomb explosion is seen here since the peak is not split.

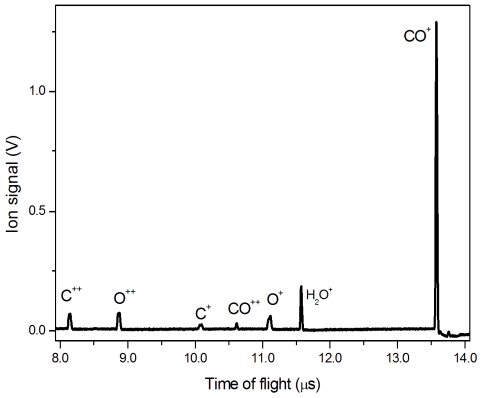

Fig. 1: TOF Mass spectrum of CO with 130 fs, 1 mJ laser pulses.

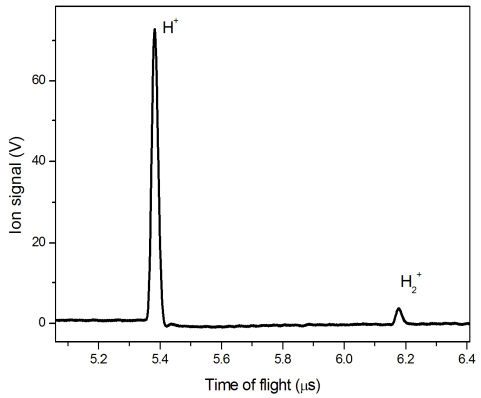

Fig. 2: TOF Mass spectrum of H_2 with 130 fs, 1 mJ laser pulses

Variation of the laser average power was done through variation of the pulse shaper power setting, and calibrated using online power measurement. The calibrated ion peak size as a function of laser intensity is thus shown for CO^+ and C^+ in Figure 3. The highest intensity corresponds to the mass spectrum in Figure 1. It is clear that the ionization process starts to saturate at intensities above $4x10^{14}$ W/cm^2. This saturation is due to most of the available molecules in the focal volume of the laser being ionized, and is well below the saturation level of the detector of the time of flight mass spectrometer. In comparison, the C^+ ion also saturates, although its threshold and saturation intensities are both higher than that of CO^+. The difference in threshold is due to the fact that C^+ is formed from CO^+ and therefore must be at the same or higher intensities.

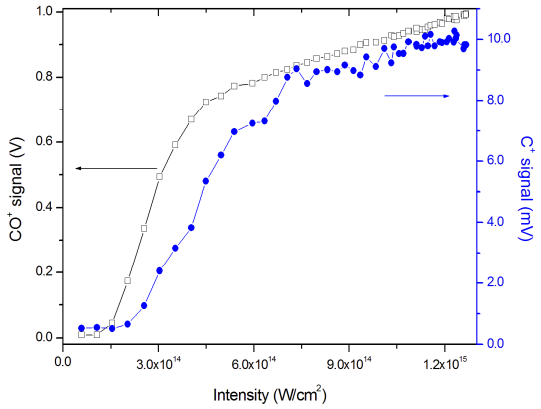

Fig. 3: Ion signals for CO^+ and C^+ as a function of laser intensity

A similar intensity variation was done on H_2 and both H_2^+ and H^+ were monitored as shown in Figure 4. In this case the H_2^+ signal has a low threshold value, a steep slope and saturates at very low values. This indicates that dissociation is dominant, although distinction cannot be made between neutral dissociation, parent ion dissociation, double ionization of the parent ion, or other possible mechanisms.

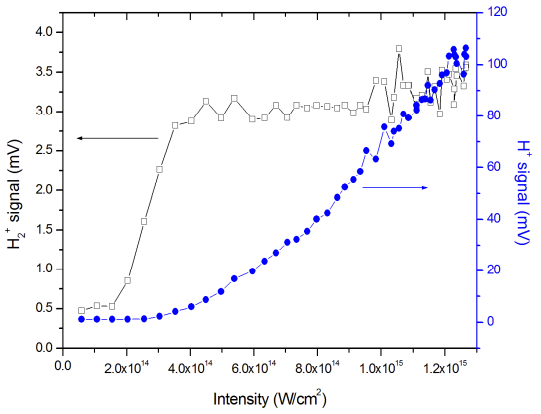

Fig. 4: Ion signals for H_2^+ and H^+ as a function of laser intensity

In this section we have demonstrated the effect of laser intensity variation on the ion fragments in the mass spectrum of CO and H_2. This includes some interesting results of interest to coherent control experimentalists. Specifically, since different molecules and ions have different ionization probabilities, some tend to ionize at lower intensities and then the ionization process is saturated at lower intensities as well (depending on the slope). This means that a ratio optimization between two species could be controlled from zero to maximum simply by tuning the laser intensity such that it lies below threshold for one species, or above saturation for another species. This is of little practical use, but could be a deciding factor in closed loop control experiments and must be considered when choosing a target function for optimization. The second point of interest is the specific result that H_2 ionization saturates at very low intensities and the

H^+ ion is dominant even at low intensities. This could be useful in chemical reaction control as this species is highly reactive.

(b) Open loop parameter scans

Open loop scans of various parameters other than intensity are possible and if differences are observed for different ion fragment species, this could point towards possible control mechanisms. For this purpose we show in Figure 5 the CO^+ and C^+ signals as a function of (a) bandwidth, (b) chirp and (c) third order phase. The results are almost identical indicating a similar process yielding both species.

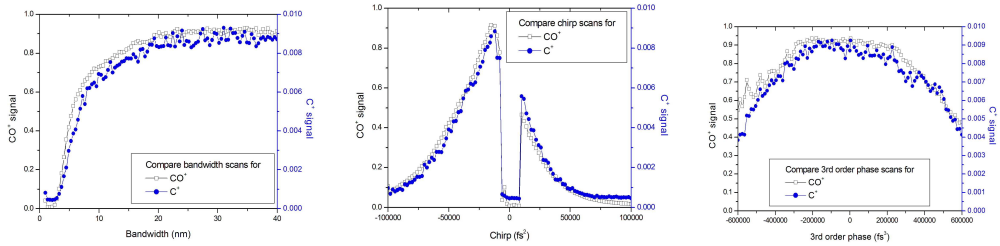

Fig. 5: Open loop scans of (a) bandwidth, (b) chirp and (c) third order phase parameter, for ion signals of CO^+ (black) and C^+ (blue).

Similarly, we monitor the CO^{++} signal compared to the C^+ signal and in this case we see differences. The CO^{++} signal increases more slowly with a bandwidth increase, meaning that the process producing this species requires a larger bandwidth and therefore a shorter pulse. Similarly, the chirp scan shows a sharper dependence on chirp for the CO^{++} species than the C^+ species. A similar result is seen on the third order phase. All these point toward the CO^{++} species being formed at higher intensities. Although this is an example of trivial intensity control, a significant variation in species formation ratios is demonstrated here.

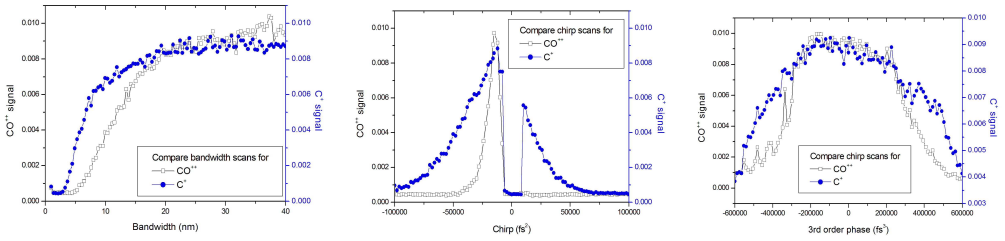

Fig. 6: Open loop scans of (a) bandwidth, (b) chirp and (c) third order phase parameter, for ion signals of CO^{++} (black) and C^+ (blue).

When analyzing the ion signals more closely, using open loop scans, it becomes apparent that the ion fragment CO^+ and C^+ have identical open loop scan dependancies on bandwidth, chirp and higher order phase. This indicates that they originate from the same physical process. In contrast, the CO^{++} ion differs considerably, and is therefore due to another physical process, possibly more nonlinear in nature. The C^+ peak is therefore attributed mainly to the dissociation of CO^+ into C^+ and O, rather than CO^{++} $\rightarrow$ $C^+ + O^+$. This illustrates the usefulness of open loop scans.

(c) Closed loop optimizations

Closed loop optimization was done using the Nelder-Mead algorithm using the nine intensity and phase controls of the Dazzler: shaping window bandwidth, central wavelength of the shaping window, a spectral hole central wavelength, width and depth, as well as the first four phase parameters in a Taylor expansion of the phase. When using the full power setting, for a near transform limited pulse, the CO^+ signal is shown in Figure (a) in black while the pulse energy photodiode signal is shown in blue. Optimization of the ratio of the CO^+ signal relative to the pulse energy resulted in the much lower pulse energy shown in (b) in blue, which produced about $2/3^{rds}$ of the CO^+ signal. The ratio improvement is 1.9 : 1.

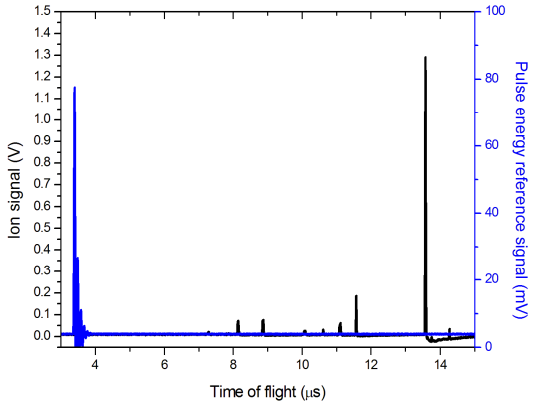

Fig. 7: Mass spectrum (black) showing CO^+ peak size as well as pulse energy (blue) due to near transform limited pulse at 700 μJ. Relative ratio CO^+ / Pulse Energy = 17.

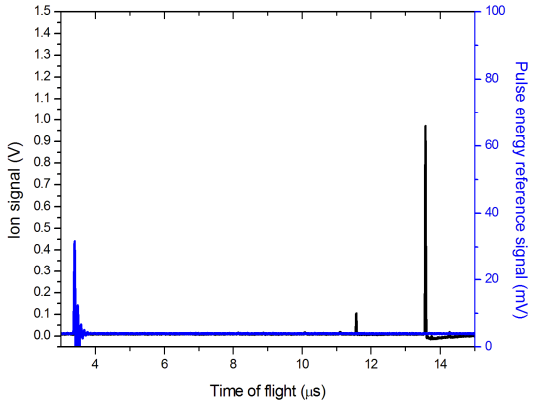

Fig. 8: Closed loop control of CO^+ / Pulse Energy producing a significant ratio improvement due to a lower pulse energy producing almost the same ion signal. Relative ratio CO+ / Pulse Energy = 32.

Closed loop optimization in exactly the same way, but this time using lower pulse energy, resulted in a slightly improved value for the CO^+ signal while the pulse energy remained the same. In this case the ratio improvement is only 1.08 : 1. The difference between the two scenarios is explained by the threshold for ionization as well as the

saturation of the ion signal. If the available pulse energy is high enough to be well above the threshold for ionization, and even in the ionization saturation regime, a smaller pulse energy will produce the same ion signal size and therefore a better ratio. In contrast, when the pulse energy is lower, a slight decrease in pulse energy will result in a decrease in ion signal, resulting in a smaller ratio (as long as saturation is not present yet). Therefore a slight improvement is found in the lower pulse energy experiment, probably due to pulse shaper improvement / cleanup of the pulse shape to produce a higher intensity. This result is important in coherent control experiments as a saturation of the ionization process occurs at different intensities for different species and can affect relative ratios and optimized pulse shapes found. What is not shown here is an anti-optimal pulse found for an optimized ratio of pulse energy to CO^+ signal. This anti-optimal pulse was found to produce very few ions at all, but still have high pulse energy. No other interesting optima where found for C^+, C^{++} or CO^{++} relative to CO^+ formation, with the current choice of search space (nine parameters).

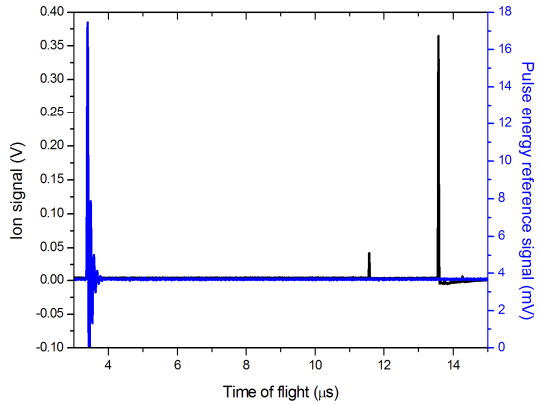

Fig. 9: Mass spectrum (black) showing CO+ peak size as well as pulse energy (blue) due to transform limited pulse at 100 μJ. Relative ratio CO+ / Pulse Energy = 21

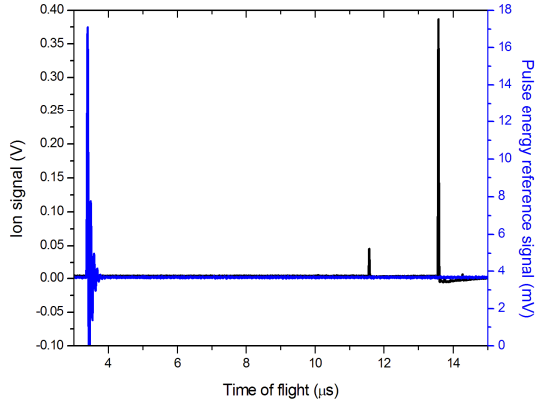

Fig. 10: Closed loop control of CO+ / Pulse Energy using 100 μJ pulse energy producing a ratio improvement of about 10%, with same pulse energy. Relative ratio CO+ / Pulse Energy = 23

(d) High pressure cell experiments

In attempts to control bimolecular chemical reactions, one difficulty is the monitoring of the production of stable products. Due to this difficulty we propose here for the first time to use pulse shapes optimized in a low pressure time of flight instrument, and apply these to a high pressure cell. We assume the pulse shape propagation is not strongly affected by the higher pressure, and the relative ratios of fragment ions are maintained even at this higher pressure. The idea is to use shaped pulses to produce different ratios of different types of fragment ions, which are very reactive and then react with other neutral and ionized species to eventually form stable reaction products. By controlling the formation of these species we could steer reactions in specific directions. In a sense this is similar to what is done by a traditional catalyst, in that bonds are broken before new bonds are formed.

A reaction cell was filled with mixtures of CO and H_2 at room temperature and pressure, and various pulses applied to this cell, following which analysis was done using time of flight mass spectroscopy and gas chromatography. Sampling was done with a needle syringe for both analytical techniques. In the time of flight, a Swagelok connector with rubber septum was used at the inlet of the TOF, before a needle valve which was used to control the pressure and to set this pressure after introducing the sample gas, to $1x10^{-6}$ mbar.

Fig. 11 shows the formation of CO_2 as a stable reaction product, and this was confirmed by GC analysis as shown in Fig. 12. Since this product could potentially be formed by C + CO → CO_2, without the need for H_2, we did a similar experiment using only CO in the chamber. Surprisingly, we found no evidence for this product (not shown), indicating that H_2 plays some role in this high intensity laser induced reaction. We suggest that the efficient formation of H^+ ions and accompanying electrons (as shown in the previous section), contribute to increase the number of collisions between species and therefore raise the effective temperature.

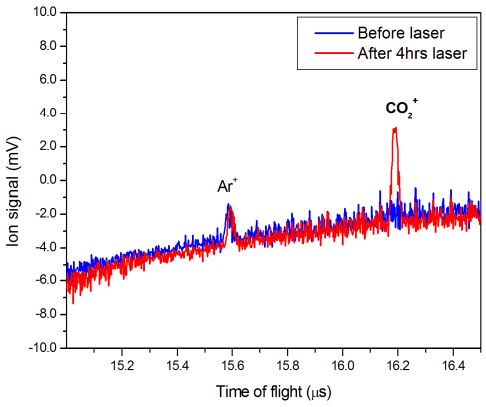

Fig. 11: Long exposure high intensity pulse irradiation of a CO and H_2 gas mixture at 1 bar and room temperature, analysed by laser ionization TOF. Production of stable CO_2

reaction product is demonstrated.

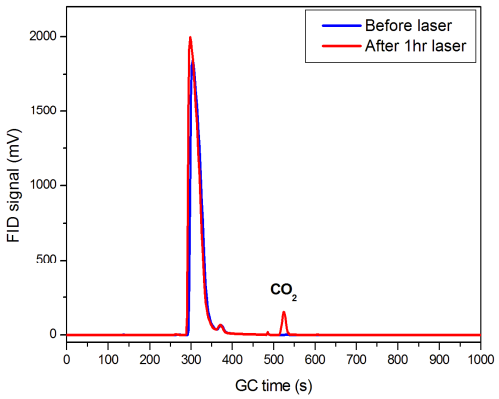

Fig. 12: CO_2 reaction product is confirmed by Gas Chromatography.

We also show evidence for C-H bond formation in Fig. 13: we observe CH^+ and CH_3^+ after a long irradiation time. These are not known to be stable products and the most likely explanation is the formation of stable CH_4 followed by laser dissociative ionization resulting in the observation of these peaks. CH_4^+ cannot be observed here due to the overwhelming O^+ signal at the same time of flight.

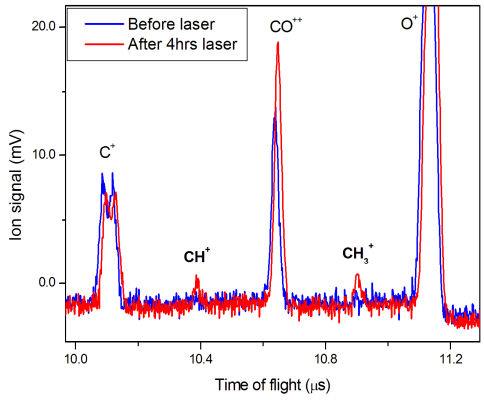

Fig. 13: Long exposure irradiation using high intensity pulse shows some evidence for C-H bond formation.

Another exciting result is the evidence for C-C bond formation shown in Fig 14, since $C_2H_2^+$ is clearly observed. The result shows that some C-C bond formation has taken place, resulting in the observation of this peak. The most likely stable product is C_2H_4 (a double carbon bond) which overlaps in the mass spectrum with the strong CO peak. Whichever the stable product, C-C bond formation is demonstrated here for the first time with laser irradiation.

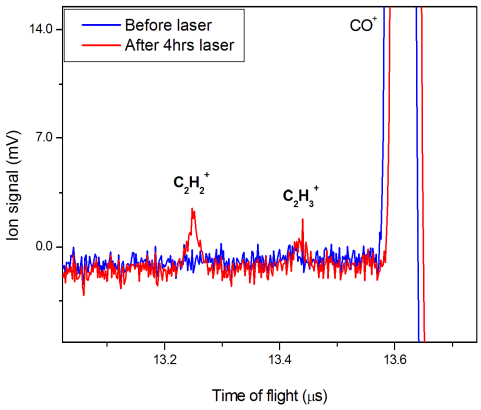

Fig. 14: Long exposure irradiation using high intensity pulse shows some evidence for C-C bond formation.

Not shown here are experiments conducted with an anti-optimal pulse for ion formation. A pulse was optimized to produce a large ratio of pulse energy relative to CO^+ signal, and this highly chirped pulse was found to produce very few ions at all yet the same pulse energy. This was applied to the reaction cell as above, and produced no new products, as expected. This proves that the process is induced by a high intensity laser induced process and not simply by heating by the energy in the pulse. Intermediate intensities produced smaller peak sizes of the same CO_2 product. As an example of this, see Figure 15 below where the resulting CO_2^+ peak from three separate hour-long exposures of fresh sample gas at 0, 340 and 640 μJ pulse energies are shown. The reason for a non-zero signal in this experiment was a more sensitive detector setting than previous experiments, indicating traces quantities of CO_2 also present in the sample gas. In contrast to the increase in CO_2^+ with irradiation intensity, the Ar^+ peak stays the same size. This argon is due to contamination in the reaction cell since argon is present at levels of 1% in atmospheric air.

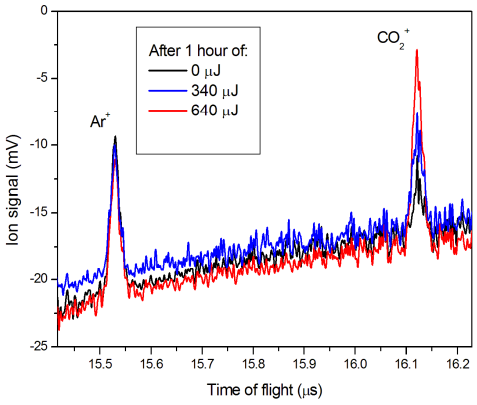

Fig. 15: Comparison between 1 hour of no irradiation (black), intermediate intensity irradiation (blue) and high intensity irradiation (red). CO_2^+ signal increase while

background Ar^+ signal unchanged.

Conclusions

We have studied the dissociative ionization of CO and H_2 and found optimized pulses for the formation of CO^+ relative to pulse energy for both low and high energy regimes. We explain the optimized high energy solution pulse as due to the saturation of the ionization process resulting in many potential solutions at lower intensities. We also found a pulse optimized for the inverse ratio, thereby producing very few ions at all, but still having high pulse energy. With the current setup we found no other significant variations in ion signals relative to one another, probably due to the limited shaping capability employed (nine amplitude and phase parameters). Future work involves searching for more variations in ion fragment ratios using full shaping of the spectral amplitude and phase. Application of these pulses to a high pressure reaction cell resulted in the formation of stable reaction products, although in very small quantities. The most clearly identified species was found to be CO_2. This peak was strongest with longest exposure times, highest intensities and not visible at all without H_2 present in the cell, or with an inverse pulse producing high pulse energy but no ions. We have thus demonstrated for the first time the laser induced bimolecular chemical reaction of CO and H2 without a catalyst. Similar work by another group on a surface catalytic reaction of these reactant species also found evidence for CH, CH_3 and in addition COH and COH2. We see COH and COH2 but also see these in the gas mixture, probably due to the impurity of our gas sample which is 98% CO and not 99.999% as in the other study. This is something we will expand on in future work. We see evidence for C-C bond formation which an exciting result and indicates the potential of this technique.

Acknowledgments: Financial support from the CSIR is acknowledged, as well as technical assistance from Mr Johan Steyn.

References

Dry, M, 2002. The Fischer-Tropsch Process: 1950-2000. Catalysis Today 71, 227-241.

Jun, KW, Roh, HS, Kim, KS, Ryu, JS, Lee, KW, 2004. Catalytic investigation for Fischer–Tropsch synthesis from bio-mass derived syngas. Applied Catalysis A 259, 221-226.

Brif, C, Chakrabarti, R, Rabitz, H, 2010. Control of quantum phenomena: past, present and future. Submitted to New Journal of Physics. Arxiv.org

Brixner, T, Gerber, G, 2004. Quantum control of gas phase and liquid phase femtochemistry. Chem Phys Chem 4, 418-438.

Dantus, M, Lozovoy, VV, 2004. Experimental coherent laser control of physicochemical processes. Chem Rev 104, 1813-1859.

Lozovoy, VV, Dantus, M, 2006. Laser control of physicochemical processes; experiments and applications. Annu Rep Prog Chem C 102, 227-258.

Du Plessis, A, Strydom, CA, Botha, LR, 2010. Comparitive study of the dissociative ionization of 1,1,1-trichloroethane using nanosecond and femtosecond laser pulses. Int J Mol Sci 11, 1114-1140.

Crim, FF, 1996. Bond-Selected Chemistry: Vibrational State Control of Photodissociation and Bimolecular Reaction. J Phys Chem 100, 12725-12734.

Bartels, RA, 2002. Coherent control of atoms and molecules. PhD thesis, University of Michigan.

Nuernberger, P, Wolpert, D, Weiss, H, Gerber, G, 2010. Femtosecond quantum control of molecular bond formation. PNAS 107, Nr 23.